

CYLINDRICAL B-SPLINE MODEL FOR REPRESENTATION AND FITTING OF HEART SURFACES

Ting-ting Jiang, S. Y. Chen, Qiu Guan and Chunyan Yao

College of Information Engineering, ZheJiang University of Technology, HangZhou China

Dept of Informatics, University of Hamburg, Hamburg Germany

Keywords: Model representation, fitting, human heart, cylindrical B-Spline, three-dimensional model.

Abstract: Heart diseases cause high mortality while the therapy of these diseases is still faulty. Consequently recovery of human's heart is valuable for clinical diagnosis and treatment. This paper proposes a new approach for three-dimensional (3-D) representation of external surface of human hearts based on B-Spline model. The model is represented in both Cartesian and cylindrical coordinates. By comparison, we find that the cylindrical coordinate is more convenient and much closely fits the structure of human hearts. The fitting is based on a cloud of points which can be extracted from computed tomography (CT) slices by an edge detection method. Results show that cylindrical B-Spline with a given number of control points can well fit the external surface of an artificial heart, which can then be further used for quantitative and functional analysis of the heart easily and accurately.

1 INTRODUCTION

Research shows heart diseases are the leading cause of death in west countries and the rate of death are increasing each year all over the world. If all kind of those diseases were cured, human life could be much longer (Frangi, 2001). At present, imaging techniques, such as magnetic resonance imaging (MRI), ultrasound, CT, and X-ray, provide noninvasive methods to study internal organs in vivo. Visualization of heart has the capability to improve the diagnostic value of cardiac images. Firstly, many diseases are strongly correlated to the shape of heart; Secondly, due to the development of medicinal imaging techniques, much more useful cardiac information has been provided while clinical diagnosis and treatment of cardiac diseases become more complexity; thirdly, it is the first step to get the other parameters.

Several techniques have been used to construct stereo hearts; however, most of the clinical information for detailed study is still constrained to two dimensions. In order to solve this problem, Pentecost et al (1999) use non-uniform rational B-Spline contours to form embryonic heart surface model (Fig.1) and the control points of the contours are identified and outlined manually at each section.

The whole surface is not continuous at all though the contours are smooth and continuous. Park et al (2003) use finite element methods to represent heart model (Fig.2 right). A static, comprehensive end-diastolic cardiac surfaces including four cardiac chambers and connected vasculature are presented as a triangular mesh (Cristian et al, 2006). Recently, one of the traditional cardiac models is called VTP model, heart and left ventricle (LV). Surface can be viewed in preview by vtp document, but this software only connects two adjacent points by lines, which will lead the surfaces, and it is imprecise to compute other cardiac parameters. A mass of attention dedicated to modeling LV model because many functional parameters are connected with LV. Though this paper constructs heart surface, we will describe the methods used to model the LV surface in the following text. They maybe good ways to recovery heart surface even the whole heart. Cardiologists used simplified shapes to approximate the LV In the early days, for example, Vuille and Weyman (1994) and Dulce et al (1993) use simple ellipsoidal models. However, since it is imprecise and can offer only few diagnostic parameters. Recently, three-dimensional surface models and correlative computer vision or graphics techniques have been developed to capture the shape and the other parameters from medical image data (Park et al,

1996). These models are finite element model, physics-based elastic model, bending and stretching model and B-Spline model etc. Most of those models are based on simple geometric models. Here gives the brief introduction of some models. Cauvin et al (1993) approximate the LV as a truncated bullet, which is much more close to the real structure of LV compared to an ellipsoid. Chen et al (1995) apply superquadrics to model the LV. Staib and Duncan (1996) use sinusoidal basis functions for shape recovery. Haber (2001) gives a 3-D finite element model, LV was divided into 16 bicubic Hermite finite elements, although it can provide clinically important information, it is still coarse. Guo Luo et al (2004) use b-spline model to construct the LV (fig.2 left) shape but the LV is considered as a generalized prolate spheroid.

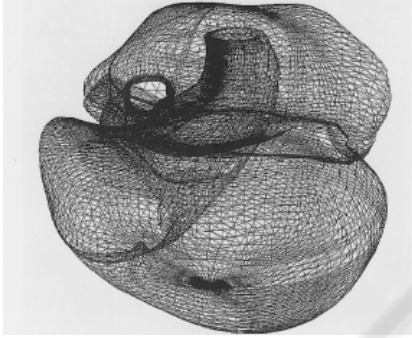


Figure 1: Representation of the embryonic heart reconstructed by NURBS contours (after Pentecost).

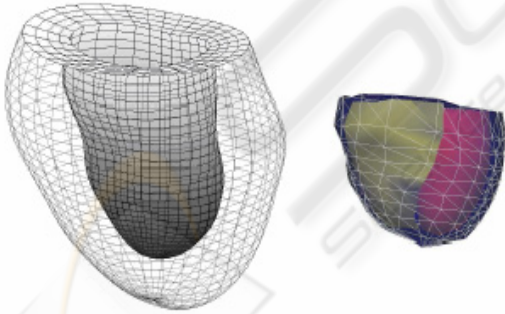


Figure 2: LV model with prolate spheroid fitting by B-Spline (left). A finite element model uses a generic heart model to generate a single model (right) (Luo and Park).

Recently, some attention has been given to surface reconstruction with the introduction of B-Spline. B-Spline, were introduced by DeBoor (1978), Ateshian (1993) uses B-spline least-squares surfaces-fitting method to create geometric models of diarthrodial joint articular surfaces. The results

prove this method is precise, flexible. Farin (2002), Farin and Dianne (2000) and Rogers (2001) present B-Spline surfaces in CAD. B.Zhang (2004) represents a human head with bi-cubic B-Spline technique and Klingensmith (2002) uses B-Spline to model lumen and vessel surfaces. And all the papers above show that B-Spline surface is a very useful technique for representing and constructing 3-D objects.

In this paper, we apply B-Spline to recovery the shape of a heart. Since B-Spline fitting makes the surface smooth and continuous. This method doesn't make use of geometrical shape of heart, but using an edge detection method to gain the external surface points from CT slices of a heart, and we use B-Spline to fit the heart surface from the achieved points. This restructured B-Spline surface is much more smooth and close to the actual data, and is domain partition. This paper introduces the theory of B-Spline curves and B-Spline surfaces in Cartesian and Cylindrical coordinates. Section three shows the characteristics of B-Spline model and some parameters which will be analyzed by this B-Spline model. The performance of the B-Spline method to recovery of a heart and the results are given in section four. Section five gives the conclusions and suggestions for further studies.

2 B-SPLINE

The B-Spline is widely used in 3-D computer graphics to describe three-dimensional surface, therefore it is fit for a variety of industrial and anatomical shapes (Amini et al, 2001), (Nicholas et al, 2003) and (Paul et al, 2001). In this section, we will describe B-Spline model detailedly and a cylindrical B-Spline model will be proposed to restructure heart surface.

2.1 B-Spline Curve in Cartesian Coordinate

A B-Spline curve of order k is expressed as:

$$\vec{P}(u) = \sum_{i=0}^n \vec{V}_i N_{i,k}(u) \quad (1)$$

Where $\vec{V} = [\vec{V}_0, \vec{V}_1, \dots, \vec{V}_n]$ are the sequence of control points of B-Spline curve, the number of control points is much fewer than a sampling of the curve

$\vec{P}(u)$ on a pixel grid and \vec{V}_i rarely reside on the actual curve (De Boor, 1978). $(n+1)$ is the number of control points in the u directions, $N_{i,k}(u)$ depending on the knot vector $U=[u_0, u_1, \dots, u_{n+k+1}]$ is B-Spline basis function of degree k , here $k < n$, because when $k=n$ B-Spline basis function becomes Bezier basis function, and when $k > n$ knot vector isn't existent. $N_{i,k}(u)$ is indicated by the following equations:

$$\begin{aligned} k=0: \\ N_{i,0}(u) &= \begin{cases} 1 & \text{if } u_i \leq u < u_{i+1} \\ 0 & \text{otherwise} \end{cases} \\ k>0: \\ N_{i,k}(u) &= \frac{u-u_i}{u_{i+k}-u_i} N_{i,k-1}(u) + \frac{u_{i+k+1}-u}{u_{i+k+1}-u_{i+1}} N_{i+1,k-1}(u) \end{aligned} \quad (2)$$

According to equation (2) Basis function $N_{i,k}(u)$ is defined by $k+2$ knots $u_i, u_{i+1}, \dots, u_{i+k+1}$ which are from U in equation (3).

When k is an even:

$$U = \left\{ \underbrace{0, \dots, 0}_{k+1}, \frac{\left(\sum_{j=1}^{k/2} l_j\right) + \frac{l_{k/2+1}}{2}}{L}, \frac{\left(\sum_{j=1}^{k/2+1} l_j\right) + \frac{l_{k/2+2}}{2}}{L}, \dots, \frac{\left(\sum_{j=1}^{n-k/2-1} l_j\right) + \frac{l_{n-k/2}}{2}}{L}, \underbrace{1, \dots, 1}_{k+1} \right\} \quad (3)$$

When k is an odd number:

$$U = \left\{ \underbrace{0, \dots, 0}_{k+1}, \frac{\sum_{j=1}^{(k+1)/2} l_j}{L}, \frac{\sum_{j=1}^{(k+1)/2+1} l_j}{L}, \dots, \frac{\left(\sum_{j=1}^{n-(k+1)/2-1} l_j\right)}{L}, \underbrace{1, \dots, 1}_{k+1} \right\}$$

Where $l_i = |\vec{V}_i - \vec{V}_{i-1}|$, $L = \sum_{i=1}^n l_i$.

2.2 B-Spline Surface in Cartesian Coordinate

A 3D B-Spline surface of degree p in the u direction and degree q in the v direction is defined as a piecewise ratio of B-Spline polynomials as given by the following function:

$$\vec{S}(u, v) = \sum_{i=0}^n \sum_{j=0}^m \vec{P}_{i,j} N_{i,p}(u) N_{j,q}(v) \quad (4)$$

where: \vec{S} is a point on the surface defined in Cartesian coordinates (x, y, z) , u and v are usually representing longitude and latitude respectively, $n+1$ and $m+1$ are the number of control points in the u and v directions respectively, $\vec{P}_{i,j}$ is the $(n+1) \times (m+1)$ matrix of control points defined in Cartesian coordinates (x_{ij}, y_{ij}, z_{ij}) . $N_{i,p}(u)$ and $N_{j,q}(v)$ are the basic functions in the u and v direction using degree p and q .

One of important properties of B-Spline is Local Modification Scheme, for example $N_{i,p}(u)$ and $N_{j,q}(v)$ is zeros when (u, v) is outside of the rectangle $[u_i, u_{i+p+1}) \times [v_j, v_{j+q+1})$ and is non-zero on $[u_i, u_{i+p+1}) \times [v_j, v_{j+q+1})$. From this property, we know that if one control point is moved to a new location, the following figure show that only the neighboring area on the surface of the moved control point changes shape and elsewhere is unchanged.

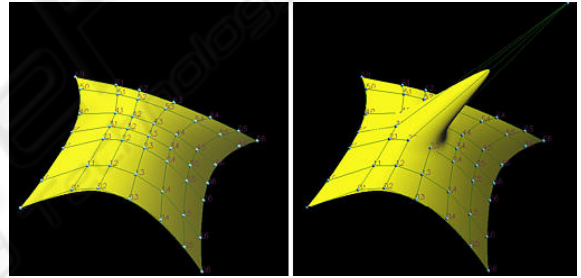


Figure 3: Left is the B-Spline surface, and right is the B-Spline surface that one control point is moved to a new location.

2.3 B-Spline Surface in Cylindrical Coordinate

Cylindrical B-Spline model more closely matches the shape of heart than Cartesian model (Deng et al, 2004) (Fig. 10). Also, it is more convenient for us to compute volume and analyze other parameters of human hearts. Consequently, it is necessary to introduce how to construct such surfaces.

In the similar way to the Cartesian case, a B-Spline surface can be defined in a system of cylindrical coordinates (r, θ, z) . In order to get the B-Spline equation in cylindrical coordinates, there are two steps necessary to do:

Step 1: coordinate transform (Javier, 1995) and (Bae, 2002)

The given $n \times m$ matrix of control points (x_{ij}, y_{ij}, z_{ij}) in 3D Cartesian coordinates are transformed into cylindrical coordinate points $(r_{ij}, \theta_{ij}, z_{ij})$ ($i = 1 \dots n, j = 1 \dots m$).

Where

$$r_{ij} = \sqrt{x_{ij}^2 + y_{ij}^2},$$

$$\theta_{ij} = \begin{cases} \pi/2 & \text{if } x_{ij} = 0 \text{ and } y_{ij} > 0 \\ 3\pi/2 & \text{if } x_{ij} = 0 \text{ and } y_{ij} < 0 \\ \text{atan}(y_{ij}/x_{ij}) & \text{if } x_{ij} > 0 \text{ and } y_{ij} \geq 0 \\ \pi + \text{atan}(y_{ij}/x_{ij}) & \text{if } x_{ij} < 0 \\ 2\pi + \text{atan}(y_{ij}/x_{ij}) & \text{if } x_{ij} > 0 \text{ and } y_{ij} < 0 \end{cases} \quad (5)$$

$$z_{ij} = z_{ij}$$

Step 2: B-Spline surface formulation

The form of the surface is similar with that have been given in equation (1), and the surface has the following system:

$$r(u, v) = \sum_{i=0}^n \sum_{j=0}^m r_{ij} N_{i,p}(u) N_{j,q}(v)$$

$$\theta(u, v) = \sum_{i=0}^n \sum_{j=0}^m \theta_{ij} N_{i,p}(u) N_{j,q}(v) \quad (6)$$

$$z(u, v) = \sum_{i=0}^n \sum_{j=0}^m z_{ij} N_{i,p}(u) N_{j,q}(v)$$

3 ANALYSIS OF B-SPLINE MODEL

B-Spline surface model has several characteristics: 1) the model can be controlled flexibility, that is to say low degrees surface and several control points can fit a wished surface, this surface is more realistic than those based on solid geometry or simple mathematical relationships. 2) It is a smooth and continuous model. 3) The model can be modified locally without changing the shape in a global way. This trait can be explained by one property of B-Spline that is local modification scheme which is introduce in section 2.2, moreover, if fine-tuning surface shape is required, one can insert more knots (and therefore more control points) so that the affected area could be restricted to a very narrow region. 4) It has a property called affine Invariance, this property states that when we want to apply a geometric or even affine transformation to the B-Spline surface, we can apply the transformation to

control points which is quite easy, and once the transformed control points are obtained the transformed B-Spline surface is the one defined by these new points, we use this characteristic to get the Cylindrical B-Spline equation.

As the purpose of getting the B-Spline model is to be further used for functional analysis and visualization of the heart convenient and exact. The final cylindrical B-Spline model will be further used for calculating cardiac functional parameters. In practice, assessment of cardiac function still relies on simple global volumetric measures like left ventricular volume (LVV) and mass (LVM) and ejection fraction (EF). As many parameters physician interested rely on LV model which can be obtained in the same way. In the following paragraphs, we will introduce some basic parameters relying on this LV model:

LVV is a basic parameter, which is necessary to obtain other important parameters, like EF. There are two general methods have been used to represent the LVV, one regards the LVV as the volume of a truncated ellipse. The other uses the sum of multiple smaller volumes of several slices. But the accuracy is not enough, especial using the truncated ellipse to replace the LV. Because of the accuracy of B-Spline model, LVV would be measured much close to the actual LVV with the application of B-Spline surface model, which will improve the future diagnosis. This is also the goal for further study.

LVM is usually normalized to total body surface area or weight in order to facilitate interpatient comparisons. The normal value of LVM normalized to body weight is $2.4 \pm 0.3/\text{kg}$ (Frangi, 2001). LVM can be calculated by following equation:

$$LVM = \rho \times (V_{epi} - V_{endo}) \quad (7)$$

Where ρ is the density of the muscle tissue (1.05 g/cm^3) (Frangi, 2001), and V_{epi} is the total volume contained within the epicardial borders of the ventricle and V_{endo} is the volume of the chamber.

The next parameter is EF which is considered as one of the most meaningful measures of heart pump function and can be got by the expression provided below.

$$EF = \frac{EDV - ESV}{EDV} \times 100\% \quad (8)$$

Where EDV is the end-diastolic volume and ESV is the end-systolic volume.

4 EXPERIMENTS AND RESULTS

4.1 Data Acquisition

First, with a given number of bitmap images which correspond to CT slices of an artificial heart, this paper uses a cardiac model to explain the good effect of B-Spline fitting which is also fit for reconstructing LV and other shape. The artificial heart is positioned on top of a wooden base and is deformable by means of oil filled syringes which are embedded under the cardiac surface. CT slices of the heart were acquired under 3 deformation levels called level_1, level_2 and level_3. The heart was at complete rest while each one of the 3 CT scans was performed. The experiment demonstrated in this section is to use level_1.

Second, extract a cloud of 3D points from the CT slices. This process can be divided into six parts:

- 1) Smooth the images by a filter.
- 2) Stitch the CT slices in the right order into a single entity according to the provided index files.
- 3) Define a Region of Interest (ROI) window in order to maintain the segmentation within a desired area (Fig. 4). This process bases on simple intensity threshold, segment the external cardiac surface from the rest of the heart.
- 4) Get the grey from the images and calculate slopes of changes of the grey. Here we define the point which have maximal slope is the border.
- 5) Extract a cloud of 3D points.
- 6) Remove some noises points from the extracted points manually.
- 7) View the result (Fig. 6)

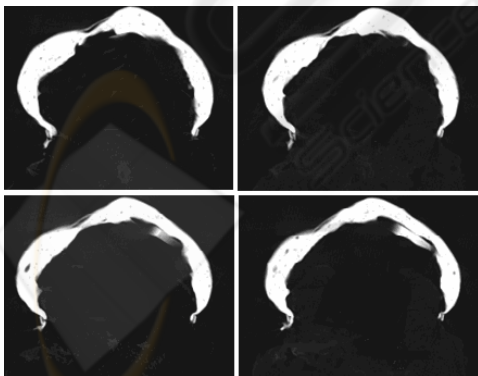


Figure 4: Four images which are the ROI areas are segmented from CT slices.

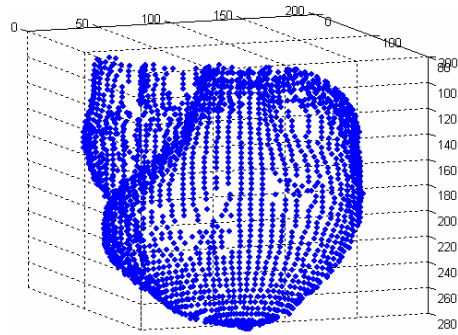


Figure 5: Discrete cardiac surface.

4.2 2-D B-Spline Curve Fitting

Figure 7 provides 20 points which come from a CT slice as the control points for B-Spline, compared this image with figure 6, we can see the outer contour of the CT slice is expressed by those discrete points. Figure 9 shows the result of using B-Spline curve with the degree of 2 to fit the CT slice and the dots in the picture are the 20 points, according to this picture we can see that almost all the control points are near the curve, that is to say the curve is fitted precisely by B-Spline.

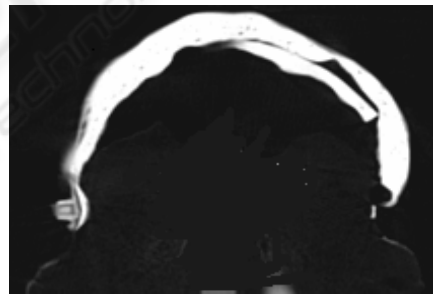


Figure 6: A segmented CT slice which is used to explain the 2-D B-Spline fitting.

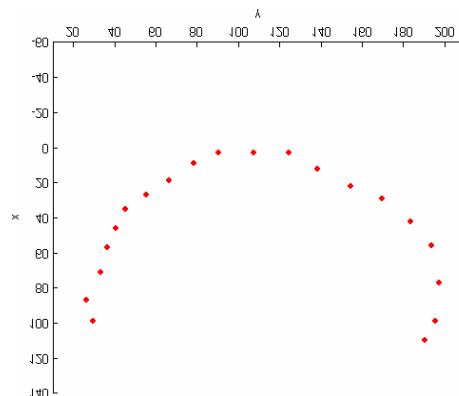


Figure 7: Twenty points from external contour of the slice given in Figure 6.

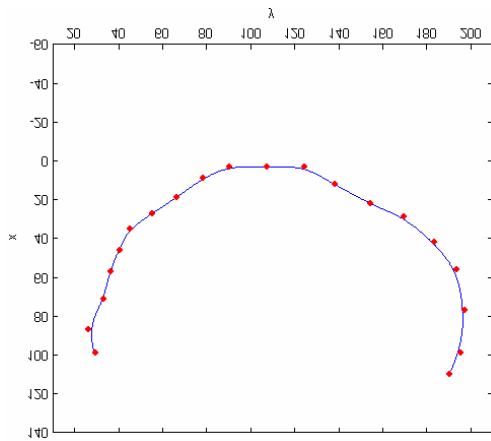


Figure 9: A b-spline curve of the slice.

4.3 3-D B-Spline Surface Fitting

The 3-D surfaces (Fig. 9 and 10) are from 2-D contours, 2-D curves are blended together to form a 3-D surface, the 2-D points in planes are splined horizontally and this horizontal curves are splined vertically to create a 3-D surface, this process is rely to the two basis functions. The control points extracted from part 4.1 are arrange in a $n \times m$ matrix, each row of the matrix are the points from a slice, n is the number of points on each slice and m is the number of slices (here $n=25$ and $m=40$). In the following parts, we will analyze Cartesian and Cylindrical model respectively, and finally compare the two models.

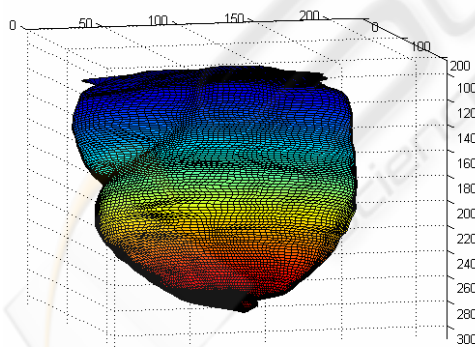


Figure 10: The Cartesian B-Spline surface fitted from the cloud of points generated in our lab.

1) Cartesian B-Spline surface. Figure 9 displays the result of using 3-D Cartesian B-Spline of degree 3 in the u direction and degree 3 in the v direction to represent the surface of the heart from the CT data set compared to the current B-Spline model based on prolate spheroid and the FE model. From Figs.1, 2, 5

and 9, it is proved that the B-Spline surface in this paper is more closely to the real model and it is continuous and smooth while the prolate spheroid-based B-Spline given in Fig. 2 left (Guo Luo et al, 2004) is not precise enough and the FE model (Park, 2003) is imprecise and not continuous. As we know, the purpose of modeling, one is for viewing the shape, and the other is for further analyzing functional parameters. The B-Spline model is more likely to compute the parameters accurately.

2) Cylindrical B-Spline surface. Figure 10 shows the surface of the heart using 3-D Cylindrical B-Spline of degree 3 in u and degree 3 in v just the same degrees as the Cartesian model. The control points which are the same points given in Cartesian model are changed into new points with all value of x subtract 66 and all value of y subtract 124.5. This change don't influence the shape of heart but let line $(0, 0, z)$ be the axis of the heart, and then translating the new points into Cylindrical coordinate points (see equation 6).

3) Comparing Fig. 9 with Fig. 10, there is noobvious difference between the two images, however cylindrical B-Spline models are more closely to the original shape at the bottom of the heart. In conclusion, cylindrical B-Spline model is more convenient and much closely fits the structure of human hearts and it is more convenient to get the clinically important parameters.

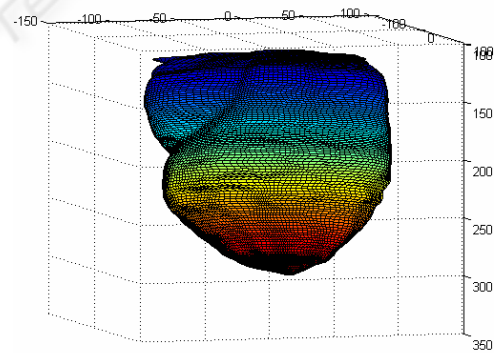


Figure 11: The Cylindrical B-Spline surface created from the same data set.

5 CONCLUSIONS

In this paper, we proposed an efficient method for representation and visualization of 3D external surfaces of heart. A heart model was reconstructed both in Cartesian and Cylindrical coordinates. By contrast, cylindrical coordinate is more convenient and much closely fits the structure of human hearts.

Further studies show cylindrical B-Spline can also be used to fit the LV and the RV, even a vivid heart might be represented by B-Spline model in the future. It is valuable for the diagnoses of heart diseases, and series of ongoing studies related on cardiac analysis are being performed depending on this result, and thus the cylindrical B-Spline model will be very useful for us in working out functional parameters of human hearts.

ACKNOWLEDGEMENTS

The testing image set was provided by Prof. G. Yang's research group at the Imperial College London. This work was supported by the National Natural Science Foundation of China [NSFC-60405009, 60605013], [ZJNSF-Y105101, Y104185], and a grant for Key Research Items from the Dept of Science and Technology of Zhejiang Province [2006C21002]. S. Y. Chen is a research fellow of the Alexander von Humboldt Foundation, Germany.

REFERENCES

- A. F. Frangi, W. J. Niessen, M. A. Viergever, 2001. Three-Dimensional Modeling for Functional Analysis of Cardiac Images: A Review. *IEEE transactions on medical imaging*, Vol.20.
- J. O. Pentecost, J. Icardo, and K. L. Thornburg, 1999. 3D computer modeling of human cardiogenesis. *Computerized Medical Imaging and Graphics*.
- K. Park, D. Metaxas, L. Axel, 2003. A Finite Element Model for Functional Analysis of 4D Cardiac-Tagged MR Images. *Lecture Notes in Computer Science*, vol. p491-498.
- Cristian Lorenz, Jens von Berg, 2006. A comprehensive shape model of the heart, *Medical Image Analysis*.
- C. Vuille and A. E. Weyman, 1994. Left ventricle I: General considerations, assessment of chamber size and function. in *Principles and Practice of Echocardiography*, 2nd ed.
- M. C. Dulce, G. H. Mostbeck, K. K. Friese, G. R. Caputo, and C. B. Higgins, 1993. Quantification of the left ventricular volumes and function with cine MR imaging: Comparison of geometric models with three dimensional data. *Radiology*, vol. 188, no. 2, pp. 371-376.
- Jinah Park, Dimitri Metaxas, 1996. Deformable Models with Parameter Functions for Cardiac Motion Analysis from Tagged MRI Data. *IEEE Trans. Medical Imaging*, 15(3): 278 ~ 289.
- J. C. Cauvin, J. Y. Boire, M. Zanca, J. M. Bonny, J. Maublant, and A. Veyre, 1993. 3D modeling in myocardial 201TL SPECT. *Computerized Medical Imaging and Graphics*, vol. 17, no. 4-5, pp. 345-350.
- C. W. Chen, J. Luo, K. J. Parker, T. S. Huang, 1995. CT volumetric data-based left ventricle motion estimation: An integrated approach. *Computerized Medical Imaging and Graphics*, vol. 19, no. 1, pp. 85-100.
- L. H. Staib, J.S. Duncan, 1996. Model-based deformable surface finding for medical images. *IEEE Trans. Med. Imag.*, vol. 15, pp. 720-731.
- Idith Haber, Ron Kikinis and Carl-Fredrik Westin, 2001. Phase-drive finite element model for spatio-temporal tracking in cardiac tagged MRI. *Springer-Verlag Berlin Heidelberg*.
- Guo Luo and Pheng Ann Heng, 2004. LV Shape and Motion: B-Spline Based Deformable Model and Sequential Motion Decomposition *IEEE Trans. Inf Technol Biomed*.
- De Boor, 1978. *A practical guide to splines*. Springer. Berlin
- Farin, G.E., 2002. *Curves and Surfaces for CAGD: A Practical Guide*. Kaufmann, San Francisco.
- Farin, G.E., Dianne, H., 2000. *The Essentials of CAGD*. Peters, Natick, USA.
- Rogers, D.F., 2001. *An Introduction to NURBS with Historical Perspective*. Morgan Kaufmann, San Francisco.
- Ateshian, G.A., 1993. A B-Spline least-squares surface-fitting method for articular surfaces of diarthrodial joints. *J. Biomech. Eng.* 115, 366-373.
- B.Zhang, J.F.M. Molenbroek, 2004. Representation of human head with bi-cubic B-Spline technique based on the laser scanning technique in 3D surface anthropometry. *Applied ergonomics*, Elsevier.
- Jon D. Klingensmith, D. Geoffrey Vince, 2002. B-Spline methods for interactive segmentation and modeling of lumen and vessel intravascular ultrasound. *Computerized Medical Imaging and Graphics. Pergamon*.
- Nicholas J. Tustison, Victor G. Dávila-Román, and Amir A. Amini. 2003. Myocardial Kinematics From Tagged MRI Based on a 4-D B-Spline Model. *IEEE Trans. on BIOMEDICAL ENGINEERING*, Vol. 50.
- Amir A. Amini, Yasheng Chen, Mohamed Elayyadi, , Petia Radeva, 2001. Tag Surface Reconstruction and Tracking of Myocardial Beads from SPAMM-MRI with Parametric B-Spline Surfaces. *IEEE Transactions Medical Imaging*.
- William Paul Segars 2001. Development and application of the new dynamic nurbs-based cardiac-torso (NCAT) phantom. University of North Carolina, MA.
- Xiang Deng and Thomas S. Denney, Jr. 2004. Three-Dimensional Myocardial Strain Reconstruction From Tagged MRI Using a Cylindrical B-Spline. *IEEE Trans. on MEDICAL IMAGING*, Vol. 237.
- Javier Sánchez-Reyes, 1995. Quasilinear parametric surfaces. *Computer-Aided Design*, Vol.27, p263 - 275.
- Seok-Hyung Bae, Byoung K. Choi. 2002. NURBS surface fitting using orthogonal coordinate transform for rapid product development. *Computer-Aided Design*. vol. 34, p683-690.